Excitation of the Slichter mode by collision with a meteoroid or pressure variations at the surface and core boundaries

Séverine Rosat, Yves Rogister

▶ **To cite this version:**

Séverine Rosat, Yves Rogister. Excitation of the Slichter mode by collision with a meteoroid or pressure variations at the surface and core boundaries. Physics of the Earth and Planetary Interiors, 2012, 190, pp.25-33. 10.1016/J.PEPI.2011.10.007 . hal-00673280

HAL Id: hal-00673280
https://hal.science/hal-00673280

Submitted on 24 Feb 2012

HAL is a multi-disciplinary open access archive for the deposit and dissemination of scientific research documents, whether they are published or not. The documents may come from teaching and research institutions in France or abroad, or from public or private research centers.

L'archive ouverte pluridisciplinaire **HAL**, est destinée au dépôt et à la diffusion de documents scientifiques de niveau recherche, publiés ou non, émanant des établissements d'enseignement et de recherche français ou étrangers, des laboratoires publics ou privés.

Excitation of the Slichter mode by collision with a meteoroid or pressure variations at the surface and core boundaries

S. Rosat, Y. Rogister

Institut de Physique du Globe de Strasbourg, UMR 7516 CNRS – Université de Strasbourg (EOST) - 5 rue Descartes, 67084 Strasbourg, France

Abstract

We use a normal-mode formalism to compute the response of a spherical, self-gravitating anelastic PREM-like Earth model to various excitation sources at the Slichter mode period. The formalism makes use of the theory of the Earth's free oscillations based upon an eigenfunction expansion methodology. We determine the complete response in the form of Green's function obtained from a generalization of Betti's reciprocity theorem. Surficial (surface load, fluid core pressure), internal (earthquakes, explosions) and external (object impact) sources of excitation are investigated to show that the translational motion of the inner-core would be best excited by a pressure acting at the core boundaries at time-scales shorter than the Slichter eigenperiods.

Keywords: Slichter mode; outer and inner core; extraterrestrial object impact

1. Introduction

The three free translational oscillations of the inner core, the so-called Slichter modes (Slichter, 1961), have been a subject of observational contro-

versy since the first detection by Smylie (1992) of a triplet of frequencies that he attributed to the Slichter modes. This detection has been supported by Courtier et al. (2000) and Pagiatakis et al. (2007) but has not been confirmed by other authors (Hinderer et al., 1995; Jensen et al., 1995; Rosat et al., 2006; Guo et al., 2007). Also, it motivated additional theoretical studies (Crossley, 1992; Rochester and Peng, 1993; Rieutord, 2002; Rogister, 2003). The search for the Slichter modes was invigorated by the development of worldwide data recorded by superconducting gravimeters (SGs) of the Global Geodynamics Project (Hinderer and Crossley, 2000). Thanks to their long-time stability and low noise level, these relative gravimeters are the most suitable instruments to detect the small signals that would be expected from the Slichter modes (Hinderer et al., 1995; Rosat et al., 2003, 2004).

The theory is now better understood and computation predicts eigenperiods between 4 and 6 h (Rogister, 2003) for the seismological reference PREM (Dziewonski and Anderson, 1981) Earth model. A more recent study by Grinfeld and Wisdom (2010) states that the period could be much shorter because of the kinetics of phase transformations at the inner-core boundary (ICB).

The observation of the Slichter modes is fundamental because, the restoring force being Archimedean, their periods are directly related to the density jump at the ICB. This parameter is still poorly known: by analyzing seismic PKiKP/PcP phases, Koper and Pyle (2004) found that it should be smaller than 450 kg/m^3, later increased to 520 kg/m^3 (Koper and Dombrovskaya, 2005), whereas Masters and Gubbins (2003) obtained 820 ± 180 kg/m^3 from normal modes observation. Tkalčic et al. (2009) have shown that the un-

certainties associated with the seismic noise might partially explain such discrepancies for the estimates of the ICB density contrast. Gubbins et al. (2008) have proposed a model with a large overall density jump between the inner and outer cores of 800 kg/m^3 and a sharp density jump of 600 kg/m^3 at the ICB itself. Such a model satisfies both the constraints set by powering the geodynamo with a reasonable heat flux from the core, and PKP travel-times and normal mode frequencies. The value of the density jump at ICB for the PREM model is 600 kg/m^3.

This paper aims at evaluating the possible amplitude of the Slichter modes for various types of excitation sources.

The seismic excitation has been previously studied by Smith (1976), Crossley (1992) and Rosat (2007). They have shown that the best natural focal mechanism to excite the Slichter mode is a vertical dip-slip source. The largest magnitude event in the past was the 1960 Chile earthquake with a magnitude $M_w = 9.6$ for the main shock. A foreshock occurred with a magnitude of 9.5 (Kanamori and Cipar, 1974). The combination of both events leads to a seismic source of magnitude $M_w = 9.8$ which would be enough to excite the Slichter modes to the nanoGal level. However, at such frequencies, the noise levels of SGs are of several nGal, even for the quietest sites (Rosat and Hinderer, 2011). Earthquakes are therefore not the most suitable source to excite the Slichter modes to a level sufficient for the SGs to detect the induced surface gravity effect.

Surficial pressure flow acting in the core has been considered by Greff-Lefftz and Legros (2007) as a possible excitation source. In this work, we reconsider the pressure flow acting in the core using a Green function formal-

ism for a non-rotating anelastic PREM Earth model. Then, we investigate the surface load and meteoroid impact as possible sources of excitation of the Slichter modes.

2. Green function formalism

We consider a spherical non-rotating anelastic Earth model. The displacement $\mathbf{u}$ at a point $\mathbf{r}$ and time t produced by any body force density $\mathbf{f}$ acting in volume V and surface force density $\mathbf{t}$ acting upon surface S can be written as a convolution of the impulse response G with the entire past history of the forces $\mathbf{f}$ and $\mathbf{t}$ (Dahlen and Tromp, 1998):

$$\mathbf{u}(\mathbf{r},t) = \int_{-\infty}^{t}\int_{V} G(\mathbf{r},\mathbf{r}';t-t')\mathbf{f}(\mathbf{r}',t')dV'dt' + \int_{-\infty}^{t}\int_{S} G(\mathbf{r},\mathbf{r}';t-t')\mathbf{t}(\mathbf{r}',t')d\Sigma'dt', \tag{1}$$

where $\mathbf{r}'$ is the integrated position vector. This relation is inferred from Betti's reciprocity relation in seismology (Aki and Richards, 1980). Seismic Green's tensor G of a non-rotating anelastic Earth is given in terms of the normal-mode complex frequencies $\nu_k = \omega_k(1+\frac{i}{2Q_k})$ and eigenfunctions $\mathbf{s}_k$ by

$$G(\mathbf{r},\mathbf{r}';t) = \Re\sum_{k}(i\nu_k)^{-1}\mathbf{s}_k(\mathbf{r})\mathbf{s}_k(\mathbf{r}')e^{i\nu_k t}H(t), \tag{2}$$

where $\Re$ denotes the real part of the complex expression and $H(t)$ is the Heaviside function.

Tromp and Mitrovica (1999) have generalized Betti's reciprocity relation to a representation theorem suited for surface-load problems, so that the displacement $\mathbf{u}$ due to a surface load σ located at $\mathbf{r}'$ is given by

$$\mathbf{u}(\mathbf{r},t) = \int_{-\infty}^{t}\int_{S} \sigma(\mathbf{r}',t')\mathbf{\Gamma}(\mathbf{r},\mathbf{r}';t-t')d\Sigma'dt', \tag{3}$$

where $\mathbf{\Gamma}$ is the surface-load Green's vector defined by

$$\mathbf{\Gamma}(\mathbf{r}, \mathbf{r}'; t) = -[G(\mathbf{r}, \mathbf{r}'; t) \cdot \nabla' \Phi(\mathbf{r}') + \mathbf{g}(\mathbf{r}, \mathbf{r}'; t)], \tag{4}$$

∇' is the gradient with respect to $\mathbf{r}'$, Φ is the unperturbed gravitational potential, and $\mathbf{g}$ is

$$\mathbf{g}(\mathbf{r}, \mathbf{r}'; t) = \Re \sum_k (i\nu_k)^{-1} \phi_k(\mathbf{r}) \mathbf{s}_k(\mathbf{r}') e^{i\nu_k t} H(t), \tag{5}$$

ϕ_k denoting the perturbation of the gravitational potential associated with the normal mode $\{\mathbf{s}_k, \phi_k\}$. Green's tensor $\{G, \mathbf{g}\}$ represents the complete point-source response.

A spheroidal mode of harmonic degree l and order m and radial overtone number n can be decomposed into three components in spherical coordinates:

$${}_n\mathbf{s}_l^m(\mathbf{r}) = {}_nU_l^m(r) Y_l^m(\theta, \phi)\hat{\mathbf{r}} + k^{-1} {}_nV_l^m(r) \frac{\partial Y_l^m}{\partial \theta}\hat{\theta} + k^{-1} {}_nV_l^m(r) \frac{1}{\sin\theta} \frac{\partial Y_l^m}{\partial \phi}\hat{\phi}, \tag{6}$$

where $Y_l^m(\theta, \phi)$ are the real spherical harmonics of degree l and order m (Dahlen and Tromp, 1998), $k = \sqrt{l(l+1)}$ and $\hat{\mathbf{r}}$, $\hat{\theta}$ and $\hat{\phi}$ are the usual unit vectors of the spherical coordinates. The associated perturbation of the gravitational potential has the form

$${}_n\phi_l^m(\mathbf{r}) = {}_nP_l^m(r) Y_l^m(\theta, \phi). \tag{7}$$

The eigenfunctions ${}_nU_l^m(r)$, ${}_nV_l^m(r)$ and ${}_nP_l^m(r)$ are functions of the radius only. Because the model is non-rotating and spherically symmetric, the $2l+1$ eigenfrequencies for each fixed l and n are degenerate into a single eigenfrequency that we can therefore denote by ${}_n\nu_l$. The summation over k in Eqs (2) and (5) is actually a triple summation over l, m and n. Since the eigenfrequencies do not depend on m, the summation over m can be performed

using the addition theorem for surface spherical harmonics, with the result [Dahlen and Tromp (1998), Eqs 10.28 and 10.34]:

$$G(\mathbf{r},\mathbf{r}';t) = \Re \sum_n \sum_l \frac{2l+1}{4\pi} \frac{e^{i_n \nu_l t}}{i_n \nu_l} \{ {}_nU_l(r)\,{}_nU_l(r')\hat{\mathbf{r}}\hat{\mathbf{r}}' P_{l0} + k^{-1}[{}_nU_l(r)\,{}_nV_l(r')\hat{\mathbf{r}}\hat{\boldsymbol{\Theta}}' - {}_n V_l(r)\,{}_nU_l(r')\hat{\boldsymbol{\Theta}}\hat{\mathbf{r}}']P_{l1} + \frac{1}{2}k^{-2}[{}_nV_l(r)\,{}_nV_l(r')\hat{\boldsymbol{\Theta}}\hat{\boldsymbol{\Theta}}'](k^2 P_{l0} - P_{l2}) + k^{-2}[{}_nV_l(r)\,{}_nV_l(r')\hat{\boldsymbol{\Phi}}\hat{\boldsymbol{\Phi}}'](\sin\Theta)^{-1} P_{l1}\}, \quad (8)$$

where $\hat{\boldsymbol{\Phi}} = \hat{\mathbf{r}} \times \hat{\boldsymbol{\Theta}}$ and Θ is the angular distance between the receiver at $\hat{\mathbf{r}}$ and the point source at $\hat{\mathbf{r}}'$:

$$\cos\Theta = \hat{\mathbf{r}} \cdot \hat{\mathbf{r}}' = \cos\theta\cos\theta' + \sin\theta\sin\theta'\cos(\phi - \phi'). \quad (9)$$

The Slichter mode is the spheroidal mode of harmonic degree one and radial overtone number one. For a non-rotating spherical model, the three Slichter frequencies are degenerate into a single eigenfrequency. As

$$P_{10}(\cos\Theta) = \cos\Theta \quad (10)$$

and

$$P_{11}(\cos\Theta) = \sin\Theta, \quad (11)$$

the term for which $l = 1$ and $n = 1$ in Eq. (8) writes:

$${}_1G_1(\mathbf{r},\mathbf{r}';t) = \frac{3}{4\pi}\Re\{\frac{e^{i\nu}}{i\nu}[U(r)U(r')\hat{\mathbf{r}}\hat{\mathbf{r}}'\cos\Theta + \frac{1}{\sqrt{2}}(U(r)V(r')\hat{\mathbf{r}}\hat{\boldsymbol{\Theta}}' - V(r)U(r')\boldsymbol{\Theta}\hat{\mathbf{r}}')\sin\Theta + \frac{1}{2}V(r)V(r')\hat{\boldsymbol{\Theta}}\boldsymbol{\Theta}'\cos\Theta + \frac{1}{2}V(r)V(r')\hat{\boldsymbol{\Phi}}\hat{\boldsymbol{\Phi}}']\} \quad (12)$$

being understood that $\nu = {}_1\nu_1$, $U = {}_1U_1$, $V = {}_1V_1$ and $P = {}_1P_1$. For PREM, the Slichter eigenperiod is 5.42 h (Rogister, 2003) and the eigenfunctions U, V and P are plotted in Fig. A.1.

The damping rate depends on the dissipation processes involved. A summary of plausible dissipation processes is given by Greff-Lefftz and Legros (2007); Guo et al. (2007); Rosat et al. (2007). The role of the outer core viscosity has been studied by Smylie and McMillan (2000) and Rieutord (2002), the effect of a mushy zone at the ICB, by Peng (1997), the influence of the magnetic field, by Buffett and Goertz (1995) and the anelastic dissipation for the core modes, by Crossley et al. (1992). Such studies have revealed that it is unlikely that the damping factor of the Slichter mode be less than 2000, corresponding to a damping time of 144 days. In this case, the induced surface gravity perturbation should be more easily detectable by SGs. We assume, in the following, a quality factor of 2000.

Using the Green function formalism, we can compute the excitation of the Slichter mode by any body or surface forces.

3. Excitation by fluid core pressure

Observational evidence for motions in the core comes from core-sensitive seismic modes, which have periods smaller than one hour, the free core nutation, which is a rotational mode of nearly-diurnal period, and variations of the magnetic field that can be related to motions in the core with timescales larger than one year. Therefore, the dynamics of the fluid core at the Slichter frequencies lacks observational evidence. Theoretical results suggest that, at timescales smaller than one day and outside the seismic band, plausible mo-

tions are to be searched for in the turbulent convection or in the spectrum of the core.

An account of small-scale turbulence driven by convection is given by Loper (2007). The timescale may be less than one day but, because of the small characteristic length-scales, turbulence is unlikely to excite the translation of the whole inner core.

Valette (1989a,b) has shown that the inertia-gravity spectrum of an inviscid liquid core is continuous and set bounds on it. The bounds depend on both the speed of rotation and squared Brunt-Väisälä frequency. Rogister and Valette (2009) and Rogister (2010) have suggested that the rotational modes might be influenced by the continuous spectrum in which they are embedded. In particular, the nearly-diurnal free inner core nutation and long-period inner core wobble might be double or even multiple and have energy in the liquid core. Pending on the value of the squared Brunt-Väisälä frequency in the outer core, the Slichter modes could also be embedded in the continuous spectrum. Similarly to what has been found for the two rotational modes of the inner core, significant motion and pressure variation in the liquid core could accompany the Slichter modes. Although a Slichter mode with its associated motion in the liquid core should then be considered as a single normal mode, we can for simplicity assume that the pressure variations in the liquid core excite the translational motions of the inner core. This is somewhat the opposite of what Buffett (2010) did to investigate the attenuation of the free inner core nutation: he assumed that the tilt of the inner core generates shear layers in the outer core where Ohmic and viscous dissipation occur.

As Greff-Lefftz and Legros (2007), we will assume that the pressure at the CMB takes the following analytical form:

$$P^c(\theta,\,\phi,\,t) = P_0^c(\theta,\,\phi)e^{-(\frac{t-T_0}{\tau})^2}, \tag{13}$$

where T_0 is the starting time of application of the pressure, τ is the time duration of the pressure source and $P_0^c(\theta,\,\phi)$ includes three terms of harmonic degree 1:

$$P_0^c(\theta,\,\phi) = P_{10}^c\cos\theta + (P_{11}^c\cos\phi + \tilde{P}_{11}^c\sin\phi)\sin\theta. \tag{14}$$

According to Okubo and Endo (1986) and Greff-Lefftz and Legros (2007), the total force exerted at the core boundaries must vanish for the centre of mass to be kept fixed. This translates into the so-called Consistency Relation (Farrell, 1972) and imposes a relation between the pressures P^c and P^{ic} at the CMB and ICB, respectively:

$$P^{ic} = \frac{r_c^2}{r_{ic}^2}P^c. \tag{15}$$

Greff-Lefftz and Legros (2007) analytically solved the equations of the elasto-gravitational deformation (Alterman et al. , 1959) for a simple Earth model made up of three homogeneous incompressible layers and investigated the excitation of the Slichter mode by a pressure acting at the outer core boundaries. In this section, we consider the same simple excitation sources to test the Green function approach for PREM, which is a more realistic Earth model. We compute the displacement $\mathbf{u}$ by means of Eqs (1) and (12). As we are mainly interested in the surface gravity effect, we only need the radial component of the displacement:

$$u_r(r,\theta,\phi,t) = \frac{3}{4\pi}\Re\{\frac{U(r)}{i\nu}\int_{-\infty}^{t} e^{i\nu(t-t')}e^{-[\frac{t'-T_0}{\tau}]^2}dt'$$

$$[U(r_c)\int_{\rm CMB}\cos\Theta(P_{10}^c\cos\theta'+(P_{11}^c\cos\phi'+\tilde{P}_{11}^c\sin\phi')\sin\theta')d\Sigma'$$
$$-U(r_{ic})\int_{\rm ICB}\cos\Theta(P_{10}^{ic}\cos\theta'+(P_{11}^{ic}\cos\phi'+\tilde{P}_{11}^{ic}\sin\phi')\sin\theta')d\Sigma']\} \quad (16)$$

At the CMB, $d\Sigma' = r_c^2\sin\theta' d\theta' d\phi'$ and, at the ICB, $d\Sigma' = r_{ic}^2\sin\theta' d\theta' d\phi'$. Taking Eqs (9) and (15) into account, the integration over θ' and ϕ' gives:

$$u_r(r,\theta,\phi,t) = \Re\{\frac{r_c^2U(r)}{i\nu}[U(r_c)-U(r_{ic})]\int_{-\infty}^{t}e^{i\nu(t-t')}e^{-[\frac{t'-T_0}{\tau}]^2}dt'$$
$$(P_{10}^c\cos\theta+P_{11}^c\sin\theta\cos\phi+\tilde{P}_{11}^c\sin\theta\sin\phi)\} \quad (17)$$

The integral

$$I(t)=\int_{-\infty}^{t}e^{i\nu(t-t')}e^{-[\frac{t'-T_0}{\tau}]^2}dt' \quad (18)$$

is calculated in the Appendix. It gives

$$I(t)=\frac{\sqrt{\pi}}{2}\tau e^{i\nu(t-T_0)}e^{-\nu^2\tau^2/4}[1+{\rm erf}(\frac{t-T_0}{\tau}+i\frac{\nu\tau}{2})], \quad (19)$$

where erf denotes the error function. The radial displacement then becomes:

$$u_r(r,\theta,\phi,t)=-\frac{r_c^2U(r)}{\omega(1+\frac{1}{4Q^2})}[U(r_c)-U(r_{ic})][\frac{\Re\{I(t)\}}{2Q}-\Im\{I(t)\}]$$
$$(P_{10}^c\cos\theta+P_{11}^c\sin\theta\cos\phi+\tilde{P}_{11}^c\sin\theta\sin\phi), \quad (20)$$

where $\Re\{\,\}$ and $\Im\{\,\}$ respectively denote the real and imaginary parts of the expression between brackets.

The degree-l gravity variation measured by a gravimeter at the surface of the Earth r_s is the sum of three terms: the free-air gravity variation owing to the displacement of the ground in the surrounding unperturbed gravity field g_0

$$g_{\rm free}=(-4\pi G\bar{\rho}+\frac{2}{r_s}g_0)U(r_s), \quad (21)$$

the inertial acceleration of the ground

$$g_{\rm in} = -\omega_l^2 U(r_s) \tag{22}$$

and the perturbation of the gravitational attraction

$$g_{\rm pot} = 4\pi G\bar{\rho} U(r_s) + \frac{2}{r_s} P(r_s). \tag{23}$$

In these expressions, $\bar{\rho}$ is the mean density of the Earth.

The degree-1 gravity variation measured by a gravimeter is therefore

$$\begin{aligned}\Delta g(\theta,\, \phi,\, t) = & \frac{r_c^2}{\omega(1+\frac{1}{4Q^2})}[U(r_c) - U(r_{ic})] \\ & [P_{10}^c \cos\theta + P_{11}^c \sin\theta\cos\phi + \tilde{P}_{11}^c \sin\theta \sin\phi] \\ & [\frac{\Re\{I(t)\}}{2Q} - \Im\{I(t)\}][-\omega^2 U(r_s) + \frac{2}{r_s} g_0 U(r_s) + \frac{2}{r_s} P(r_s)]\end{aligned} \tag{24}$$

We consider a zonal pressure $P_{10}^c = 150$ Pa and compute the induced geocentre motion, inner-core translation and surface gravity perturbation for both $\tau = 1.5$ h and 15 h (Fig. A.2). As the centre of mass is fixed, the geocentre motion, which is the displacement of the figure centre with respect to the centre of mass, corresponds to the surface displacement (Greff-Lefftz and Legros, 1997).

For P_{10}^c varying from 0 to 1000 Pa and τ ranging from 0.1 and 10 h, we compute a 2D-map (Fig. A.3) of the surface gravity perturbation when the exciting pressure has vanished (i.e. $t > T_0 + \tau$).

Our results for the PREM model show excitation amplitudes larger by 70 % than the amplitudes computed by Greff-Lefftz and Legros (2007), who used a very simple model made up of three incompressible homogeneous layers with a solid inner core, a liquid outer core and a rigid mantle. If

we consider such a 3-layer model with the average densities of the PREM inner core, outer core and mantle, we obtain a period of 3.09 h for the Slichter mode and excitation amplitudes in close agreement with the values of Greff-Lefftz and Legros (2007). They do not provide numerical details for the structure of their model but mention that its Slichter period is 3.08 h, which is almost equal to the Slichter period of our 3-layer model. Therefore, the Green function formalism we have adopted gives the same result as the analytical solution for the degree-1 deformation of a simple 3-layer model obtained by Greff-Lefftz and Legros (2007).

The difference between the excitation amplitudes we obtain for PREM and the amplitudes computed by Greff-Lefftz and Legros (2007) comes from the different Earth models. The elasticity of the mantle and inner core, the compressibility of the outer core and the density jump at the ICB all come into play. Greff-Lefftz and Legros (2007) mention that the elasticity of the mantle perturbs the solutions by 30 %, without any further specifications. We have checked that, by making the outer core of our simple 3-layer model compressible, with a P-wave velocity of 11083 m/s, the excitation amplitude of the Slichter mode is decreased by 40 % with respect to the incompressible model. The influence of the compressiblity and stratification of the core on the Slichter mode was also investigated by Rogister (2003).

The perturbation of the surface gravity field is the largest when τ is smaller than half the Slichter eigenperiod. When τ is one fourth of the Slichter period, a 10 Pa pressure acting at the CMB, which by Eq. (15) imposes a 81 Pa pressure at the ICB, is enough to induce a 10 nGal (0.1 nm/s^2) surface gravity perturbation, which should be detectable by SGs.

4. Excitation by a surface load

A degree$-l$ surficial mass distribution σ^s at the surface r_s exerts forces over the Earth in two ways. First, at the interface between the Earth and the load σ^s, the static contact forces give rise to a degree$-l$ pressure

$$P^s = g_0 \sigma^s. \tag{25}$$

Second, the gravitational attraction of the load σ^s over the entire Earth is described by a degree$-l$ potential

$$\phi = \frac{4\pi G}{2l+1} \sigma^s r_s \begin{cases} (\frac{r}{r_s})^l \text{if r} \leq r_s \\ (\frac{r_s}{r})^l \text{if r} > r_s \end{cases} \tag{26}$$

Atmospheric pressure models are sampled at 3 h at best. So instead of using actual data, we write the surface density load in the analytical form:

$$\sigma^s(\theta,\, \phi,\, t) = \sigma_0^s(\theta,\, \phi) e^{-[\frac{t-T_0}{\tau}]^2}, \tag{27}$$

which is the same as the expression used for the fluid core pressure in Section 3. The degree-one load σ_0^s, like P_0^c, contains three terms:

$$\sigma_0^s(\theta,\, \phi) = \sigma_{10} \cos\theta + (\sigma_{11} \cos\phi + \tilde{\sigma}_{11} \sin\phi) \sin\theta. \tag{28}$$

After integration of Eq. (3) over the whole surface, the radial displacement is given by:

$$\begin{aligned} u_r(r,\theta,\phi,t) = & \frac{r_s^2 U(r)}{\omega(1+\frac{1}{4Q^2})} [U(r_s) g_0 + P(r_s)] [\frac{\Re\{I(t)\}}{2Q} - \Im\{I(t)\}] \\ & [\sigma_{10} \cos\theta + \sigma_{11} \sin\theta \cos\phi + \tilde{\sigma}_{11} \sin\theta \sin\phi], \end{aligned} \tag{29}$$

and the perturbation of the surface gravity is

$$\begin{aligned}\Delta g(t) = & \frac{r_s^2}{\omega(1+\frac{1}{4Q^2})}[U(r_s)g_0 + P(r_s)][\frac{\Re\{I(t)\}}{2Q} - \Im\{I(t)\}] \\ & [\sigma_{10}\cos\theta + \sigma_{11}\sin\theta\cos\phi + \tilde{\sigma}_{11}\sin\theta\sin\phi] \\ & [-\omega^2 U(r_s) + \frac{2}{r_s}g_0 U(r_s) + \frac{2}{r_s}P(r_s)] \end{aligned} \tag{30}$$

We use a zonal surface load pressure of 1000 Pa (the surface mass density is then $\sigma_{10} = P_{10}/g_0$) and we compute the induced geocentre motion, the inner-core translation and the surface gravity perturbation for two excitation time-scales (1.5 h and 15 h) (Fig. A.4). When applying a surface load of 1000 Pa during $2\tau = 3$ h, the induced surface gravity perturbation has an amplitude of 5 nGal (0.05 nm/s^2) corresponding to an inner-core translation of 15 mm and a geocentre motion in the opposite direction with an amplitude of 0.015 mm. When the excitation time-scale (15 h) is larger than the Slichter period, the excitation amplitude is smaller.

We also plot the surface gravity perturbation associated to the Slichter mode excited by a surface load for different excitation time-scales and various zonal pressure amplitudes in Fig. A.5. The conclusion is similar to the one for an internal pressure flow, except that the surface gravity variations are about 300 times smaller.

In this section, we have estimated the effect of a surface load on the Slichter mode. Another source that, intuitively, could make the inner core oscillate is a shock at the surface. Hence, in the next section, we study the excitation by an object impact on the Earth's surface.

5. Excitation by an object impact

Stellar objects, such as asteroids or comets, are dragged by the Earth's atmosphere and reach the Earth's surface at relatively modest velocities, typically a few tens of km/s. The released energy is comparable to nuclear explosions (according to Table 6 of Collins et al. (2005), from 3.2 to 3.9 10^8 megatons of TNT, where 1 Mt = 4.2 10^{15} J). The collisions between the Earth and the largest meteoroids, with diameters from hundreds of meters to several kilometers, blast out the impacting objects, create wide craters, generally twenty times larger than the diameter of the meteoroids, and melt terrestrial rocks. Fortunately, such collisions are rare events: statistically, a 100 to 200 m meteoroid hits the Earth every 1000 years, a 500 to 800 m meteoroid every 30000 years, and a 5 km meteoroid every 40 millions years.

We believe it is reasonable to assume that both the mass and linear momentum of the impacting object are negligible with respect to the Earth's mass and linear momentum, so the orbit of the Earth is not disturbed. Besides, the rotation period and tilt of the rotation axis of the Earth could be changed by the impact if the angular momentum of the object is large enough. We, however, consider impactors for which the angular momentum is at least one hundred times smaller than the Earth's; the change of the Earth's angular momentum is therefore negligible. The major known meteoroid impacts had such characteristics (Table A.1).

Consequently, we reduce the extraterrestrial impact issue to the computation of the equivalent seismic magnitude corresponding to the released energy. The computation proposed here is based on the equations and drastic simplifications used by Collins et al. (2005), which are summarized below.

When an object enters the Earth's atmosphere, it loses its kinetic energy through deceleration and ablation. The rate of change of the velocity v is given by the drag equation (Collins et al., 2005; Melosh, 1989):

$$\frac{dv}{dt} = -\frac{3\rho z C_D}{4\rho_i L_0} v^2, \tag{31}$$

where z is the altitude, C_D is the drag coefficient, taken equal to 2, and ρ_i and L_0 are, respectively, the impactor density and diameter. By assuming an exponential atmosphere,

$$\rho(z) = \rho_0 e^{-z/H}, \tag{32}$$

where $H = 8$ km is the scale height and ρ_0 =1 kg/m^3, the velocity of the impactor as a function of altitude is given by:

$$v(z) = v_0 \exp\left(-\frac{3\rho(z) C_D H}{4\rho_i L_0 \sin\alpha}\right), \tag{33}$$

where α is the entry angle and v_0, the velocity at the top of the atmosphere. On its trajectory down to the ground, the impactor goes through the increasing atmospheric pressure and, possibly, breaks up. Collins et al. (2005) have established an empirical strength-density relation to estimate the yield strength Y_i (in Pa)

$$\log_{10} Y_i = 2.107 + 0.0624\sqrt{\rho_i} \tag{34}$$

and give an approximate expression for the altitude of breakup $z^\star$:

$$z^\star \approx -H[\ln(\frac{Y_i}{\rho_0 v_i^2}) + 1.308 - 0.314 I_f - 1.303\sqrt{1 - I_f}], \tag{35}$$

where

$$I_f = 4.07\frac{C_D H Y_i}{\rho_i L_0 v_i^2 \sin\alpha}, \tag{36}$$

and v_i is the impactor velocity at the surface.

Equation (35) holds provided that $I_f < 1$. Otherwise, and more rarely, the object does not break up and the velocity at the impact is given by Equation (33).

Following Collins et al. (2005), we use the approximative pancake model (Chyba et al., 1993; Melosh, 1981) to describe the disintegration of the meteoroid. Let us denote by z_b the airburst altitude, which is the altitude of complete dispersion of the fragments. According to the simplifying assumptions of the pancake model, z_b is given by

$$z_b = z^\star - 2H \ln(1 + \frac{\ell}{2H}\sqrt{f_p^2 - 1}), \tag{37}$$

where ℓ is the dispersion length scale:

$$\ell = L_0 \sin\alpha \sqrt{\frac{\rho_i}{C_D \rho(z^\star)}} \tag{38}$$

and the pancake factor f_p is between 2 and 10. We shall adopt Collins et al. (2005)'s value of 7. If $z_b > 0$, the airburst occurs in the atmosphere, there is neither impact nor associated seismic event. If $z_b \leq 0$, the fragments are not dispersed when they collide with the ground and the impact velocity is:

$$\begin{aligned} v_{zr} = v(z^\star) \exp\{(-\frac{3}{4}\frac{C_D\rho(z^\star)}{\rho_i L_0^3 \sin\alpha}\frac{H^3 L_0^2}{3\ell^2}(32 + (\frac{\ell}{H})^2 e^{z^\star/H} \\ +6e^{2z^\star/H} - 16e^{3z^\star/2H} - 3(\frac{\ell}{H})^2)\} \end{aligned} \tag{39}$$

The remaining kinetic energy at the moment of impact is

$$E_{cr} = \frac{\pi}{12}\rho_i L_0^3 v_{zr}^2. \tag{40}$$

After the impact, a fraction k_s of E_{cr} is radiated as seismic waves. Experimental data (Schultz and Gault, 1975) provide $k_s \in [10^{-5}, 10^{-3}]$. We will

take $k_s = 10^{-4}$. The seismic moment being given by

$$M_0 = 2\frac{\mu}{\Delta\sigma_S} k_s E_{cr}, \tag{41}$$

where the stress release $\Delta\sigma_S \approx 3$ MPa and the rigidity $\mu = 30$ GPa, the seismic magnitude is then:

$$M_w = \frac{2}{3}\log_{10}(M_0) - 10.73 \tag{42}$$

with M_0 in dyn.cm (1 dyn.cm=10^{-7} N/m).

We compute the magnitude M_w for the different meteoroid impacts of Table A.1 and, in the same table, report the surface gravity perturbation associated with the translational excitation of the inner core. Note that the source is represented in terms of moment tensor by three orthogonal force couples (spherically symmetric explosion) and not as a vertical force. Indeed, the shock pressure would reach hundreds of gigapascals and the impact energy would vaporize the rocks and cause a spherically symmetric explosion, as observed from the spherical shape of known craters.

For the biggest meteoroid, the surface excitation amplitude of the Slichter mode is 0.0067 nm/s^2, which is less than the detection threshold of 1 nGal (= 0.01 nm/s^2). To determine what kind of impact would be necessary to excite sufficiently the Slichter mode so that it is detectable in surface gravity data, we compute the magnitude M_w and gravity perturbation Δg for various ranges of density ρ_i, velocity v_0, diameter L_0 of the object and for seismic efficiency k_s varying between 10^{-5} and 10^{-2}. The resulting maps are plotted in Fig.A.6. The shaded areas correspond to M_w larger than 9.7, which is the magnitude required for the surface gravity effect to reach the nGal detection threshold for a surficial explosive moment source (Fig. A.7).

We see from Fig.A.6 that to produce a seismic event of magnitude larger than 9.7, the size, density or velocity of the impacting object should have unrealistic huge values. However, the value of the seismic efficiency k_s has a direct impact on the equivalent seismic magnitude. For instance, with a seismic efficiency of 10^{-3} instead of 10^{-4}, a meteoroid similar to the one which produced the Chicxulub crater in Mexico would be able to induce a seismic event of such a magnitude. Of course, the consequences would have been devastating.

We conclude that the surficial seismic events, including extra-terrestrial object impacts and explosions, are not efficient to make the inner-core oscillate at the Slichter frequency with an amplitude large enough to be observed at the surface. The reason is the same as for earthquakes, i.e. the excitation amplitude is directly linked to the seismic magnitude and the radial eigenfunctions of the Slichter mode are constant and close to zero in the mantle (Crossley, 1992; Rogister, 2003; Rosat, 2007).

6. Conclusions and perspectives

We have investigated the excitation of the translational free motion of the inner core by a pressure due to a flow in the outer core and acting at both the ICB and CMB, by a surface load, which can be associated to atmospheric or oceanic loading for instance, and by the collision between the Earth and a stellar object. Our conclusion is that the Slichter mode would be best excited by a pressure acting at the core boundaries at time-scales shorter than half the Slichter eigenperiod.

For the pressure source at the ICB and CMB and the loading source at the

surface, we have considered Gaussian functions of time. More complicated sources should be considered, in particular stochastic forces produced by some turbulent flow in the core or at the surface. The stochastic excitation, be it oceanic and atmospheric, of normal modes has been studied for instance by Tanimoto and Um (1999), Tanimoto (1999, 2007) and Webb (2007, 2008). However, the time scale for the Slichter mode is larger than for the other seismic normal modes, whose eigenperiod is shorter than 1 hour, so we should consider a theory different from the Kolmogorov theory of turbulence.

We have considered an analytic expression for the surface pressure as a source for the excitation of the Slichter mode. A more realistic approach should be based on actual atmospheric data from space correlation of world-wide barometers or from weather institutes (ECMWF, NCEP...), provided the data are available at a time resolution higher than the Slichter period.

Appendix A. Evaluation of the time integral I(t) (Eq. 18)

We evaluate the following integral:

$$I(t) = \int_{-\infty}^{t} e^{i\nu(t-t')} e^{-[\frac{t'-T_0}{\tau}]^2} dt'$$

We put $b = \frac{t-T_0}{\tau}$ and introduce the variable $x = \frac{t'-T_0}{\tau}$. $I(t)$ becomes:

$$I(t) = \tau \int_{-\infty}^{b} e^{i\nu\tau(b-x)} e^{-x^2} dx = \tau \int_{-\infty}^{b} e^{i\nu\tau b} e^{-x(x+i\nu\tau)} dx$$

We perform the change of variable $y = x + i\frac{\nu\tau}{2}$:

$$\begin{aligned} I(t) &= \tau e^{i\nu\tau b} \int_{-\infty}^{b+i\frac{\nu\tau}{2}} e^{-(y-i\frac{\nu\tau}{2})(y+i\frac{\nu\tau}{2})} dy \\ &= \tau e^{i\nu\tau b} e^{-\frac{\nu^2\tau^2}{4}} \int_{-\infty}^{b+i\frac{\nu\tau}{2}} e^{-y^2} dy \end{aligned}$$

The integral $\frac{2}{\sqrt{\pi}} \int_z^{+\infty} e^{-y^2} dy$ is the complementary error function $\mathrm{erfc}(z) = 1 - \mathrm{erf}(z)$, where

$$\mathrm{erf}(z) = \frac{2}{\sqrt{\pi}} \int_0^z e^{-y^2} dy. \tag{A.1}$$

So the time integral $I(t)$ is given by:

$$I(t) = \frac{\sqrt{\pi}}{2} \tau e^{i\nu(t-T_0)} e^{-\nu^2\tau^2/4} [1 + \mathrm{erf}(\frac{t-T_0}{\tau} + i\frac{\nu\tau}{2})]$$

References

Aki, K. and Richards, P.G. (1980). Quantitative Seismology, Freeman, New York.

Alterman, Z., Jarosch, H. and Pekeris, L. (1959). Oscillations of the Earth, *Proc. Roy. Soc. Lond., Ser. A*, *2*52, 80-95.

Buffett B. A. (2010). Tidal dissipation and the strength of the Earth's internal magnetic field, *Nature*, *468*, 952–954, doi:10.1038/nature09643

Buffett, B., Goertz, D.E. (1995). Magnetic damping of the translational oscillations of the inner core, *Geophys. J. Int.*, *120*, 103-110.

Chyba, C.F., Thomas, P.J. and Zahnle, K.J. (1993). The 1908 Tunguska explosion: Atmospheric disruption of a stony asteroid, *Nature*, *361*, 40-44.

Collins, G.S., Melosh, H.J. and Marcus, R.A. (2005). Earth Impact Effects Program: A Web-based computer program for calculating the regional environmental consequences of a meteoroid impact on earth, *Meteoritics & Planetary Science*,*4*0 (6), 817-840.

Courtier, N., Ducarme, B., Goodkind, J., Hinderer, J., Imanishi, Y., Seama, N., Sun, H., Merriam, J., Bengert, B., Smylie, D.E. (2000). Global superconducting gravimeter observations and the search for the translational modes of the inner core, *Phys. Earth Planet. Int.*, *117*, 320.

Crossley, D.J. (1992). Eigensolutions and seismic excitation of the Slichter mode triplet for a fully rotating Earth model, *EOS*, *73*, 60.

414 Crossley, D.J., Hinderer, J. and Legros, H. (1992). On the excitation, detec-
415 tion and damping of core modes, *Phys. Earth Planet. Int.*, *68*, 97-116.

416 Dahlen, F.A. and Tromp, J. (1998). Theoretical Global Seismology, Prince-
417 ton: Princeton Univ. Press., Princeton, NJ, 1025 pp.

418 Dziewonski, A.M., Anderson, D.L. (1981). Preliminary reference Earth model
419 (PREM), *Phys. Earth Planet. Int.*, *25*, 297-356

420 Farrell, W.E. (1972). Deformation of the Earth by surface loads, *Rev. Geo-*
421 *phys. Space Phys.*, *10*(3), 761-797.

422 Greff-Lefftz, M. and Legros, H. (1997). Some remarks about the degree-one
423 deformation of the Earth, *Geophys. J. Int.*, *131*, 699-723.

424 Greff-Lefftz, M. and Legros, H. (2007). Fluid core dynamics and degree-one
425 deformations: Slichter mode and geocentre motions, *Phys. Earth Planet.*
426 *Int.*, *161*, 150-160.

427 Grinfeld, P. and Wisdom, J. (2010). The effect of phase transformations at
428 the inner core boundary on the Slichter modes, *Phys. Earth Planet. Int.*,
429 178, 3-4, 183-188.

430 Gubbins, D., Masters, G. and Nimmo, F. (2008). A thermochemical bound-
431 ary layer at the base of Earth's outer core and independent estimate of
432 core heat flux, *Geophys. J. Int.*, *174*, 1007-1018.

433 Guo, J.Y., Dierks, O., Neumeyer, J. and Shum, C.K. (2007). A search for the
434 Slichter modes in superconducting gravimeter records using a new method,
435 *Geophys. J. Int.*, *168*, 507-517.

436 Hinderer, J., Crossley, D. and Jensen, 0. (1995). A search for the Slichter
437 triplet in superconducting gravimeter data, *Phys. Earth Planet. Int.*, *90*,
438 183-195.

439 Hinderer, J. and Crossley, D. (2000). Time variations in gravity and infer-
440 ences on the Earths structure and dynamics, *Surv. Geophys.*, *21*, 1-45.

441 Jensen, O.G., Hinderer, J. and Crossley, D.J. (1995). Noise limitations in the
442 core-mode band of superconducting gravimeter data, *Phys. Earth Planet.*
443 *Int.*, *90*, 169-181.

444 Kanamori, H. and Cipar, J.J. (1974). Focal process of the great Chilean
445 earthquake May 22, 1960, *Phys. Earth Planet. Int.*, *9*, 128-136.

446 Koper, K.D. and Dombrovskaya, M. (2005). Seismic properties of the inner
447 core boundary from PKiKP/PcP amplitude ratios, *Earth Planet. Sci. Lett.*,
448 *237*, 680-694.

449 Koper, K.D. and Pyle, M.L. (2004). Observations of PKiKP/PcP amplitude
450 ratios and implications for Earth structure at the boundaries of the liquid
451 core, *J. Geophys. Res.*, *109*, B03301.

452 Loper D. E. (2007). Turbulence and small-scale dynamics in the core, *In*
453 Olson, P. (Ed.) Core dynamics, Vol. 2 Treatise on Geophysics, pp 187–
454 206. (Ed. Schubert, G.), Elsevier: Amsterdam.

455 Masters, G. and Gubbins, D. (2003). On the resolution of the density within
456 the Earth, *Phys. Earth Planet. Int.*, *140*, 159-167.

457 Melosh, H.J. (1981). Atmospheric breakup of terrestrial impactors. In *Multi-*
458 *ring basins*, edited by Schultz P.H. and Merrill R.B. New York: Pergamon
459 Press. pp. 29-35.

460 Melosh, H.J. (1989). *Impact cratering: A geologic process*. New York: Oxford
461 University Press. 245 p.

462 Okubo, S. and Endo, T. (1986). Static spheroidal deformation of degree I.
463 Consistency relation, stress solution and partials, *Geophys. J. R. Astron.*
464 *Soc.*, *86*, 91-102.

465 Pagiatakis, S. D., Yin, H. and Abd El-Gelil, M. (2007). Least-squares self-
466 coherency analysis of superconducting gravimeter records in search for the
467 Slichter triplet, *Phys. Earth Planet. Int.*, *160*, 108-123.

468 Peng, Z.R. (1997). Effects of a mushy transition zone at the inner core bound-
469 ary on the Slichter modes, *Geophys. J. Int.*, *131*, 607-617.

470 Rieutord, M. (2002). Slichter modes of the Earth revisited, *Phys. Earth*
471 *Planet. Int.*, *131*, 269-278.

472 Rochester, M.G. and Peng Z.R. (1993): The Slichter modes of the rotating
473 Earth: a test of the subseismic approximation, *Geophys. J. Int.*, *111*, 575-
474 585.

475 Rogister, Y. (2003). Splitting of seismic free oscillations and of the Slichter
476 triplet using the normal mode theory of a rotating, ellipsoidal earth, *Phys.*
477 *Earth Planet. Int.*, *140*, 169-182.

478 Rogister Y. (2010). Multiple inner core wobbles in a simple Earth
479 model with inviscid core, *Phys. Earth Planet. Int*, *178*, 8–15,
480 doi:10.1016/j.pepi.2009.08.012.

481 Rogister Y. & Valette B. (2009). Influence of liquid core dynamics on ro-
482 tational modes, *Geophys. J. Int.*, *176*, 368–388, doi: 10.1111/j.1365-
483 246X.2008.03996.x

484 Rosat, S., Hinderer, J., Crossley, D.J., Rivera, L. (2003). The search for the
485 Slichter mode: comparison of noise levels of superconducting gravimeters
486 and investigation of a stacking method. *Phys. Earth Planet. Int.*, *140* (13),
487 183-202.

488 Rosat, S., Hinderer, J., Crossley, D.J., Boy, J.P. (2004). Performance of
489 superconducting gravimeters from long-period seismology to tides, *J. of*
490 *Geodyn.*, *38*, 461-476.

491 Rosat, S., Rogister, Y., Crossley, D. et Hinderer, J. (2006). A search for the
492 Slichter Triplet with Superconducting Gravimeters: Impact of the Density
493 Jump at the Inner Core Boundary, *J. of Geodyn.*, *41*, 296-306.

494 Rosat, S. (2007). Optimal Seismic Source Mechanisms to Excite the Slichter
495 Mode. Int. Assoc. of Geod. Symposia, Dynamic Planet, Cairns (Australia),
496 *vol. 130*, 571-577, Springer Berlin Heidelberg New York.

497 Rosat, S., Hinderer, J. (2011). Noise Levels of Superconducting Gravimeters:
498 Updated Comparison and Time Stability, *Bull. Seism. Soc. Am.*, *vol. 101*,
499 No. 3, doi: 10.1785/0120100217

Rosat, S., Sailhac, P. and Gegout, P. (2007). A wavelet-based detection and characterization of damped transient waves occurring in geophysical time-series: theory and application to the search for the translational oscillations of the inner core, *Geophys. J. Int.*, *171*, 55-70.

Schultz, P.H. and Gault, D.E. (1975). Seismic effects from major basin formation on the moon and Mercury, *The Moon*, *12*, 159-177.

Slichter, L.B. (1961). The fundamental free mode of the Earths inner core, *Proc. Natl. Acad. Sci.*, USA, *47*, 186-190.

Smith, M.L. (1976). Translational inner core oscillations of a rotating, slightly elliptical Earth, *J. Geophys. Res.*, *81* (17), 3055-3065.

Smylie, D.E. (1992). The inner core translational triplet and the density near Earth's centre, *Science*, *255*, 1678-1682.

Smylie, D.E., McMillan, D.G. (2000). The inner core as a dynamic viscometer, *Phys. Earth Planet. Int.*, *117*, 71-79.

Tanimoto, T. (1999). Excitation of normal modes by atmospheric turbulence: source of long-period seismic noise, *Geophys. J. Int.*, *136*, 395-402.

Tanimoto, T. (2007). Excitation of normal modes by non-linear interaction of ocean waves, *Geophys. J. Int.*, *168*(2), 571582, doi:10.1111/j.1365-246X.2006.03240.x.

Tanimoto, T. and Um, J. (1999). Cause of continuous oscillations of the Earth, *J. Geophys. Res.*, *104*, 28723-28739.

Tkalčic, H., Kennett, B. L. N. and Cormier, V. F. (2009). On the inner-outer core density contrast from PKiKP/PcP amplitude ratios and uncertainties caused by seismic noise, *Geophys. J. Int.*, *179*, 425-443.

Tromp, J. and Mitrovica, J.X. (1999). Surface loading of a viscoelastic earth-I. General theory, *Geophys. J. Int.*, *137*, 847-855.

Valette B. (1989a). Spectre des vibrations propres d'un corps élastique, auto-gravitant, en rotation uniforme et contenant une partie fluide, *C. R. Acad. Sci. Paris*, **309**, Sér. I, 419–422.

Valette B. (1989b). Etude d'une classe de problèmes spectraux, *C. R. Acad. Sci. Paris*, **309**, Sér. I, 785–788.

Webb, S. C. (2007). The Earth's hum is driven by ocean waves over the continental shelves, *Nature*, *445*, 754 756, doi:10.1038/nature05536.

Webb, S. C. (2008). The Earth's hum: the excitation of Earth normal modes by ocean waves, *Geophys. J. Int.*, *174*, 542-566.

Table A.1: Some meteoroid impacts on the Earth continental crust and oceanic crust. The impact angle is supposed to be 45 degrees and the impact velocity is 20 km/s.

Location	Date (AD or My BP)	Diameter (m)	Density (kg/m^3)	M_w	Δg (nm/s^2)
Tunguska Fireball Siberia	1908 AD	60	2700 (rock)	No impact	
Ries Crater Germany	15.1 ± 0.1	1500	2700 (rock)	7.4	$3.9\ 10^{-6}$
Rochechouart France	214 ± 8	1500	3350 (stony-iron)	7.5	$4.9\ 10^{-6}$
Chesapeake Bay USA	35.5 ± 0.3	2300	2700 (rock)	7.8	$1.4\ 10^{-5}$
Chicxulub Mexico	64.98 ± 0.05	17500	2700 (rock)	9.6	$6.7\ 10^{-3}$

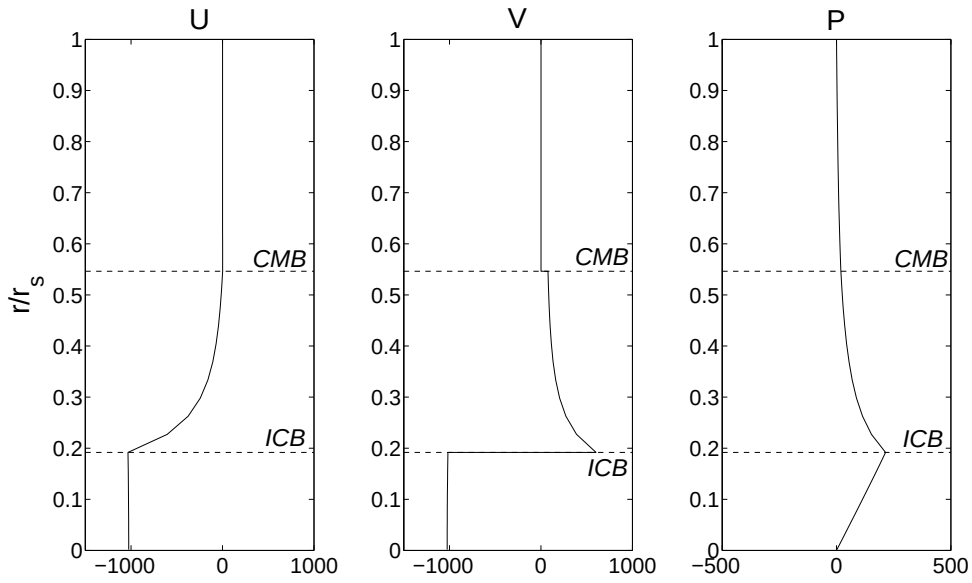

Figure A.1: Eigenfunctions of the Slichter mode ${}_1\mathrm{S}_1$ for the PREM model. The vertical axis is the radius normalized by the Earth's surface radius r_s. U and V are the radial dependence of the displacement given by Eq. (6). P is the perturbation of the gravitational potential. The normalization of the eigenfunctions is such that $U(r_s) = 1$ m.

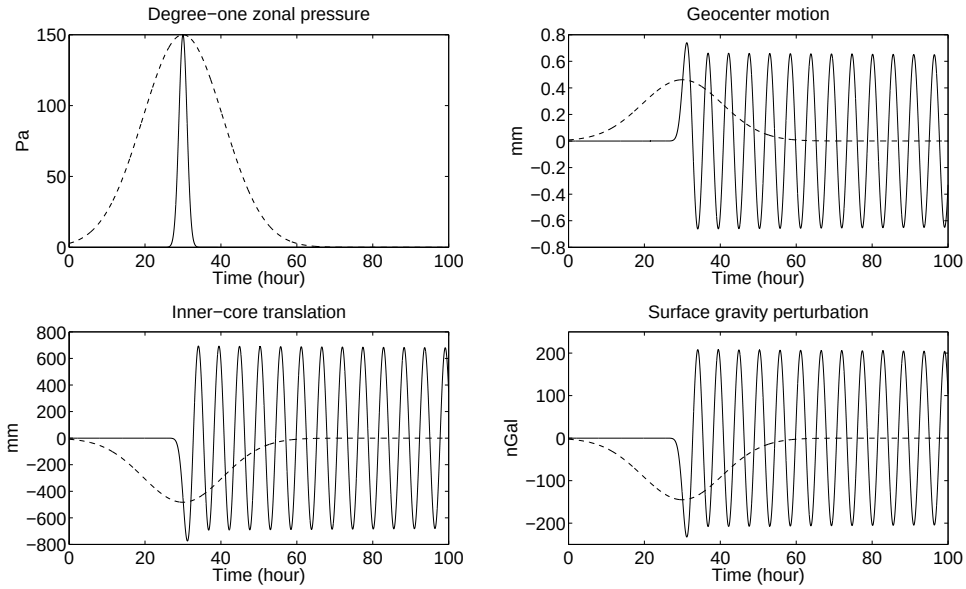

Figure A.2: Effects of the excitation of the Slichter mode by a fluid pressure acting at the CMB for two different excitation time-scales: $\tau = 1.5$ h (solid line) and $\tau = 15$ h (dashed line). This figure is similar to Fig. 3 of Greff-Lefftz and Legros (2007) but we have applied a Green tensor formalism to the PREM model. (a) Degree-one zonal pressure; (b) geocentre motion; (c) inner-core translation; (d) surface gravity perturbation.

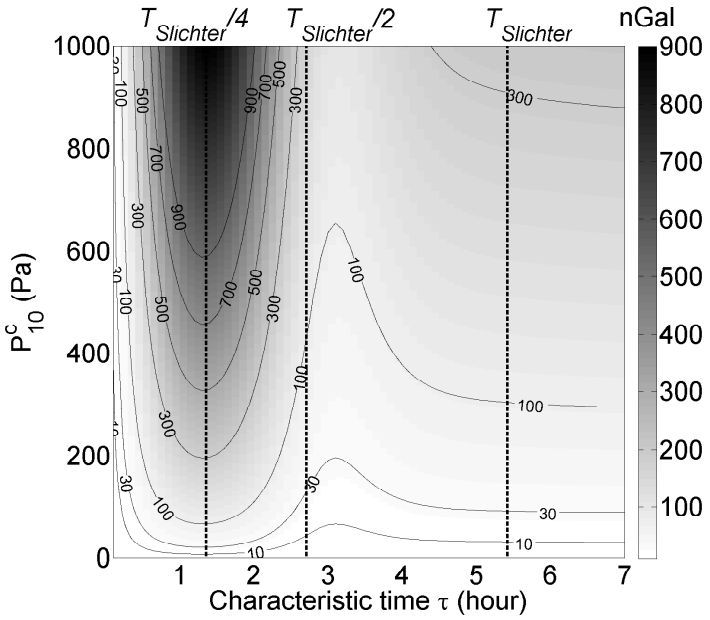

Figure A.3: Surface gravity perturbation induced by the Slichter mode excited by a fluid pressure acting at the CMB for different excitation time-scales and various zonal pressure amplitudes. The vertical dotted lines correspond to one fourth of the Slichter period, one half of the Slichter period and the Slichter period.

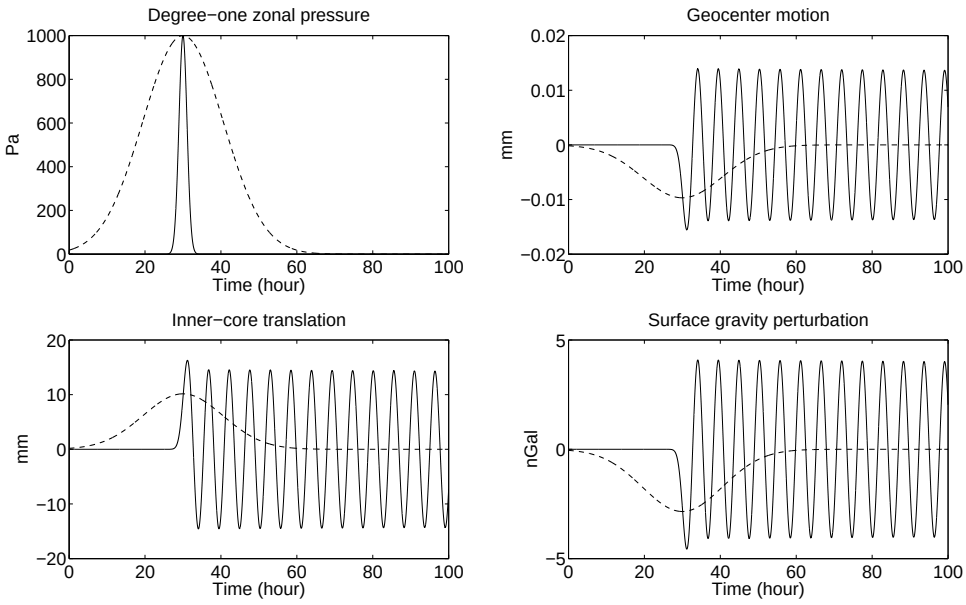

Figure A.4: Resulting effects of the excitation of the Slichter mode by a zonal surface load $\sigma(t) = \sigma_0 e^{-[\frac{t-T_0}{\tau}]^2}$ for two different excitation time-scales: $\tau = 1.5$ h (solid line) and $\tau = 15$ h (dashed line). (a) Degree-one zonal pressure effect; (b) geocentre motion; (c) inner-core translation; (d) surface gravity perturbation.

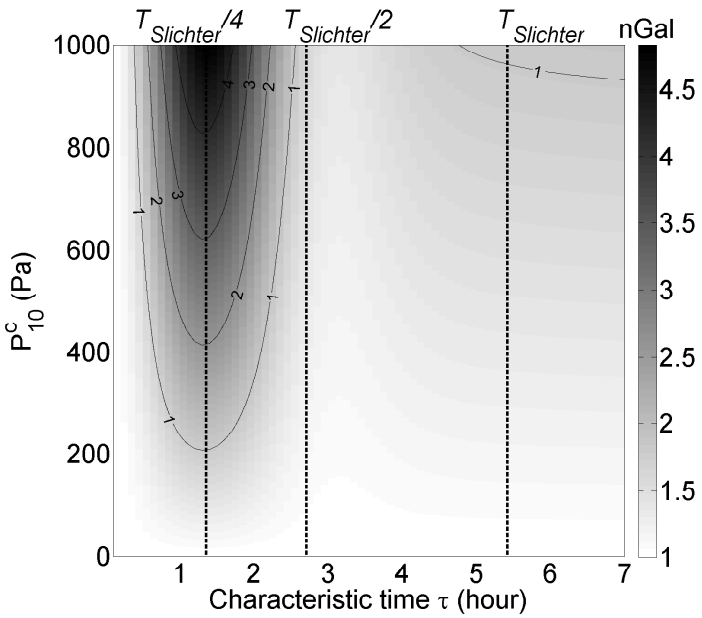

Figure A.5: Surface gravity perturbation induced by the Slichter mode excited by a surface load for different excitation time-scales and various zonal pressure amplitudes.

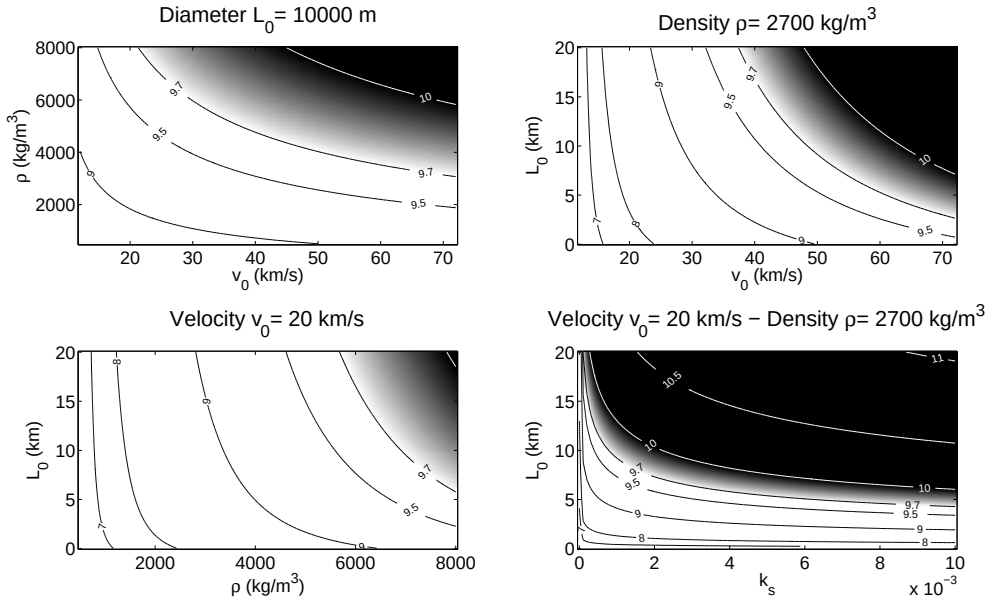

Figure A.6: Seismic magnitude as a function of the impactor parameters and seismic efficiency k_s. The shaded area corresponds to moment magnitudes larger than 9.7, i.e. to induced surface gravity perturbation larger than 1 nGal.

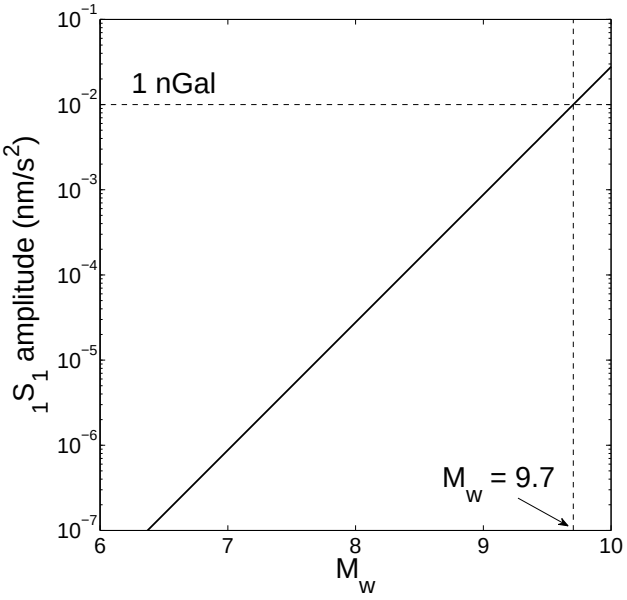

Figure A.7: Surface gravity perturbation induced by the Slichter mode as a function of the moment magnitude of a superficial energy release (explosion or object impact).